CellPress

Article

Multimodal Smart Eyewear for Longitudinal Eye Movement Tracking

Eye Tracking · Pulse Detection · Sleep Studies · Human-Computer Interaction

S. Zohreh Homayounfar, Soha Rostaminia, Ali Kiaghadi, Xingda Chen, Emerson T. Alexander, Deepak Ganesan, Trisha L. Andrew

tandrew@umass.edu

HIGHLIGHTS

Initiated chemical vapor deposition affords a reusable hydrogel electrode on fabrics

An ion-conductive fabric electrode measures pulse waveforms when placed on the face

Eye masks decorated with fabric hydrogel electrodes allow for wireless eye tracking

Chesma, a lightweight and tailorable mask, simultaneously tracks eye motion and pulse

We present a first-of-its-kind fabric hydrogel electrode that is reusable and washable, does not cause skin irritation, and can be continuously operated for upward of 8 h without losing signal integrity. Second, we report an ion-based fabric pressure sensor that measures pulse waveforms when placed on the face. We decorate a lightweight eye mask with these novel fabric electrodes to create a portable detection platform named "Chesma," which can wirelessly track eye motion and pulse in natural environments over long periods of time.

Demonstrate
Proof-of-concept of performance with intended application/response

4

Matter

CellPress

Article

Multimodal Smart Eyewear for Longitudinal Eye Movement Tracking

S. Zohreh Homayounfar,[1] Soha Rostaminia,[2] Ali Kiaghadi,[3] Xingda Chen,[2] Emerson T. Alexander,[4] Deepak Ganesan,[2] and Trisha L. Andrew[1,5,6,*]

SUMMARY

Contextual measurements of multiple physiological signals using familiar garments or accessories can provide insights into health and behavior. Recording these signals on or near the face is challenging because most subjects are sensitive to implements placed on the face or head. Here, fabric electrodes and garment design strategies are used synergistically to afford an unobtrusive platform, Chesma, for longitudinal acquisition of physiological signals from a user's face. Chesma contains two novel fabric-based electrodes: a hydrogel electrode (tAgTrode) that retains its ionic character after multiple uses/washes, does not cause skin irritation, and can be continuously operated for upward of 8 h without losing signal integrity. Second is an ion-conductive fabric pressure sensor (Press-ION) that captures pulse waveforms. When sewn onto a lightweight eye mask, these electrodes simultaneously gather complementary electro-oculography and cardiac data, which can enable sleep quality and psychological studies and improve the accuracy and usability of virtual reality headsets.

INTRODUCTION

The emergence of fabric-based sensors to collect physiological signals in daily life is considered a breakthrough in pervasive healthcare systems.[1–3] Embedding textile-based sensing elements into regular garments that a user is naturally inclined to wear over long periods allows us to have multiple, independent modes of signal acquisition in a given device, which leads to profound insights into health status. Here, biopotential signals, such as electrocardiography[4–12] (ECG), electro-oculography[13–15] (EOG), or electroencephalography[16,17] (EEG), are considered a significant tunneling pathway into the body.[18] In measuring biopotentials, electrodes[19,20] play a critical role as the interface through which ionic currents in the body are translated into electronic signals that can be read out with various instrumentation.

We have long known that EOG can allow us to monitor eye movement patterns, even with the eyes being closed.[21] In particular, EOG offers many advantages compared with rigid camera-based devices[22] that suffer from data accuracy issues stemming from inescapable motion artifacts and cybersecurity risks. EOG is based on measuring the corneoretinal biopotential of the eyes, which can be modeled as a constant electrical dipole. Eyeball rotation leads to a change in the dipole orientation, which subsequently gives rise to a change in the amplitude of the EOG signal. Measures of eye parameters such as saccades, fixations, blink patterns, and facial gestures can reveal important information about sleep quality, mental health,[23,24]

Progress and Potential

Unobtrusive, contextual measurements of multiple, complementary physiological signals using familiar garments or accessories can provide deep insights into health and behavior. Recording these signals on or near the face is challenging because most subjects are particularly sensitive and reactive to implements placed on the face or head. These practical considerations limit development of improved technology that can accurately monitor the ophthalmological and cardiac signals needed for studies on sleep quality and mental health. Here, we show how fabric-based electrodes and garment design methods work synergistically to afford an unobtrusive platform, Chesma, for longitudinal monitoring of pulse and eye parameters in everyday environments. Being able to track pulse and eye movement in a single wearable device will enable a host of biomedical, physiological, and psychosocial studies, in addition to improving the accuracy and usability of gaming and virtual reality headsets.

neurodegenerative diseases,[25,26] and schizophrenia,[27,28] and can improve user interfaces for augmented reality/virtual reality (AR/VR) systems.[29–32]

However, the fundamental challenge in reliably extracting biopotential signals through wearable electrodes is to design an electrode enjoying both the signal quality of traditional wet electrodes and the comfort of the dry ones. Commercially available, gold-standard wet electrodes provide reliably high signal-to-noise ratio (SNR) when used in clinical settings. The high SNR of these disposable electrodes has its roots in the presence of a salt-infused hydrogel on top of the electrode as well as a skin-irritating adhesive,[33] which minimizes the effect of motion artifacts on the signal acquisition. These electrodes are neither aesthetically pleasing nor practical for long-term wear, since once the hydrogel dehydrates, the electrode loses its functionality and should be disposed of. As a result, EOG data acquisition is almost always performed through dry electrodes. For example, silver-coated[14] or graphene-coated[34] fabrics, or polymeric foams[17] have been embedded as a dry electrode into a head cap,[35] eye mask,[14] and headband[34] to obtain EOG and EEG. Most notably, the commercial J!NSE MEME eyeglasses[15] mount three dry electrodes on the nose bridge of the glasses. These structures benefit enormously from being sleek, light, and comfortable to wear; however, due to the dry nature of their electrodes, they are highly prone to give rise to motion artifacts, even when the wearer is talking, chewing, or moving the head. For example, the motion artifacts are so intense and persistent in J!NSE MEME that facial expressions can be inferred from the signals alone.[36]

In addition, many health studies,[35,37,38] such as accurate detection of sleep stage,[39–42] call for simultaneously capturing both eye movement patterns and cardiac rhythm. However, up to now, integrating all the required sensing elements in one device seems almost impossible, specifically when it comes to textile-based wearable electronics. Therefore, the goal of this study is to develop unobtrusive eyewear embedded with fabric-based biopotential electrodes and pulse detectors for long-term contextual measurement of eye parameters and cardiac rhythm, respectively, all in a single reusable device (Figure 1).

RESULTS AND DISCUSSION

Design and Fabrication of tAgTrode

Our priority in designing a wearable bioelectrode was to combine the comfort and reusability of fabric with high SNR and low motion artifacts of wet electrodes. The first engineering problem was to have a conductive plate, as a charge collector, with an ionic interface that can effectively bridge between the ionic charges in the body and the flowing electrons in the wires. To address this issue, by obtaining inspiration from the commercial wet gel electrodes (hereafter called "reference electrode"), we used a rectangular array of silver (Ag) threads (tAgs) with base resistivity of 2 Ω/cm, embroidered on top of a hydrophobic, poly(perfluorodecyl acrylate) (PFDA)-coated[43] cotton (Figure 2A). This silver plate current collector must be further coated with silver(I) chloride (AgCl), as an ionic interface, for biopotential signal transduction. Quick bleach treatment of silver thread array oxidizes the outer surface of the silver layer (ca. 50–100 nm), transforming it into AgCl (Figures 2B and 2C). The successful formation of the AgCl layer is confirmed by the surface chemical composition data (Figure S1) revealed by X-ray photoelectron spectroscopy (XPS).

Next, we tackled the most important feature of the time-tested reference electrode, the salt-infused hydrogel, which is needed to translate ion-based biological signals

[1]Department of Chemistry, University of Massachusetts Amherst, Amherst, MA 01002, USA

[2]College of Computer Science, University of Massachusetts Amherst, Amherst, MA 01002, USA

[3]Department of Electrical Engineering, University of Massachusetts Amherst, Amherst, MA 01002, USA

[4]Springfield Technical Community College, Springfield, MA 01105, USA

[5]Department of Chemical Engineering, University of Massachusetts Amherst, Amherst, MA 01002, USA
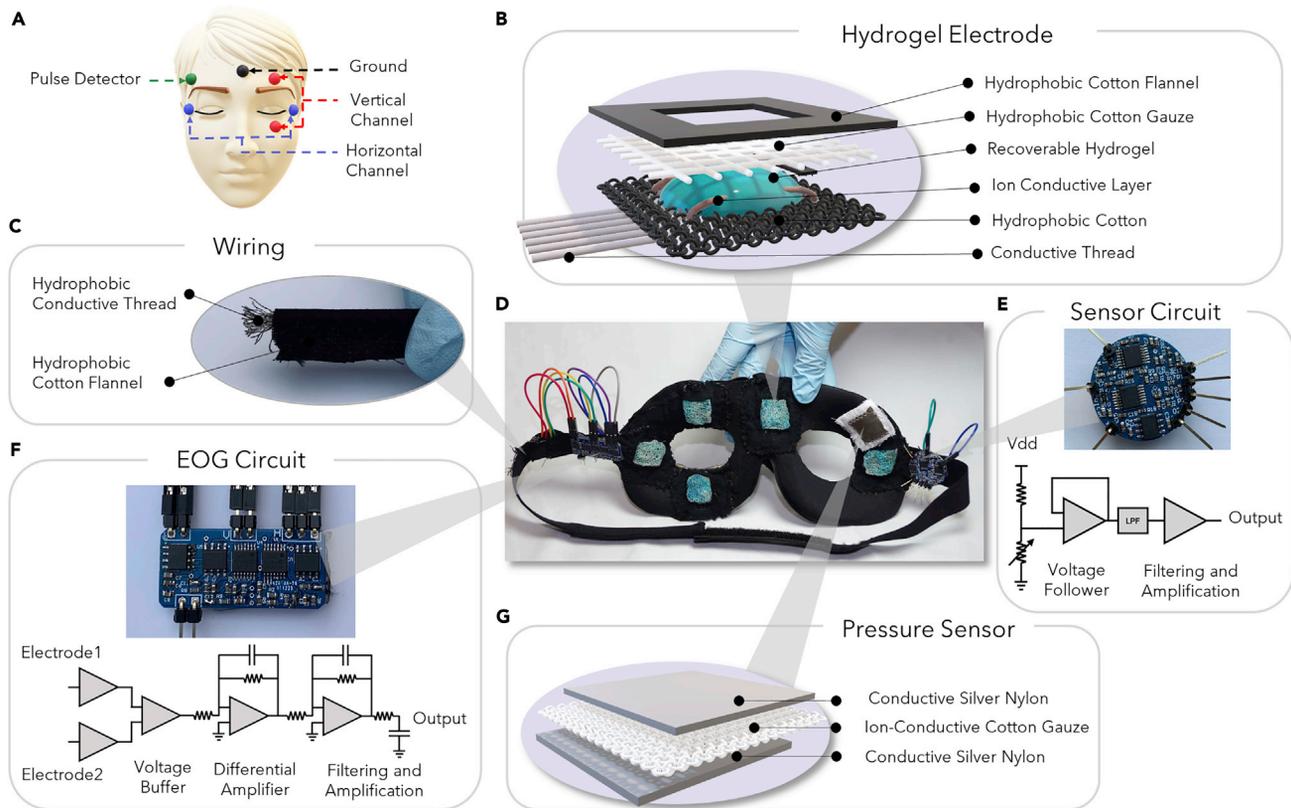
[6]Lead Contact

*Correspondence: tandrew@umass.edu

https://doi.org/10.1016/j.matt.2020.07.030

CellPress

Figure 1. Chesma: A Bimodal Sensing Platform for Acquiring Physiological Signals from the Face

Figure360▷ For a Figure360 author presentation of this figure, see https://doi.org/10.1016/j.matt.2020.07.030.

(A) Schematic for the points of data acquisition on the face, where electrodes are placed.

(B) Schematic illustration of tAgTrode electrode used for electro-oculography (EOG).

(C) Photograph of wiring constructed with hydrophic conductive threads.

(D) Photograph of a Chesma with embedded electrodes, pulse detector, microcontroller, and wiring.

(E) Photograph of the EOG controller and the equivalent circuit model.

(F) Photograph of the pressure sensor/pulse acquisition controller and its equivalent circuit model.

(G) Schematic illustration of the Press-ION pressure sensor for pulse waveform acquisition.

into an electric current, reduce motion artifacts, and minimize noise from stray electromagnetic fields. We note that it is still a significant challenge in the materials community to develop a hydrogel that can be stably grafted onto an underlying surface, maintain a constant baseline ion concentration, and, most importantly, be rehydrated and reused after being dried out. To address these issues and design a stable hydrogel as the solid-state electrolyte in our fabric bioelectrode, we took advantage of a vapor-phase process called initiative chemical vapor deposition (iCVD),[44] the schematic for which is shown in Figure 2E. iCVD is an efficient, solvent-free method that involves simultaneous synthesis and deposition of poly(acrylate) films at reduced pressures and is particularly useful for coating textured, porous, and/or solvent-swollen substrates, such as textiles and gels.[44] Here, we use iCVD to serve two purposes: first, to create a reusable composite hydrogel out of poly(2-hydroxyethylacrylate) (pHEA) and a pharmaceutical-grade silver gel formulation, and second, to enable grafting of this composite hydrogel to the underlying PFDA-coated cotton backing layer.

To transform this aqueous mixture into a persistent, rubbery, and rehydratable composite hydrogel, we coat it with pHEA using iCVD. pHEA is chosen because it forms a
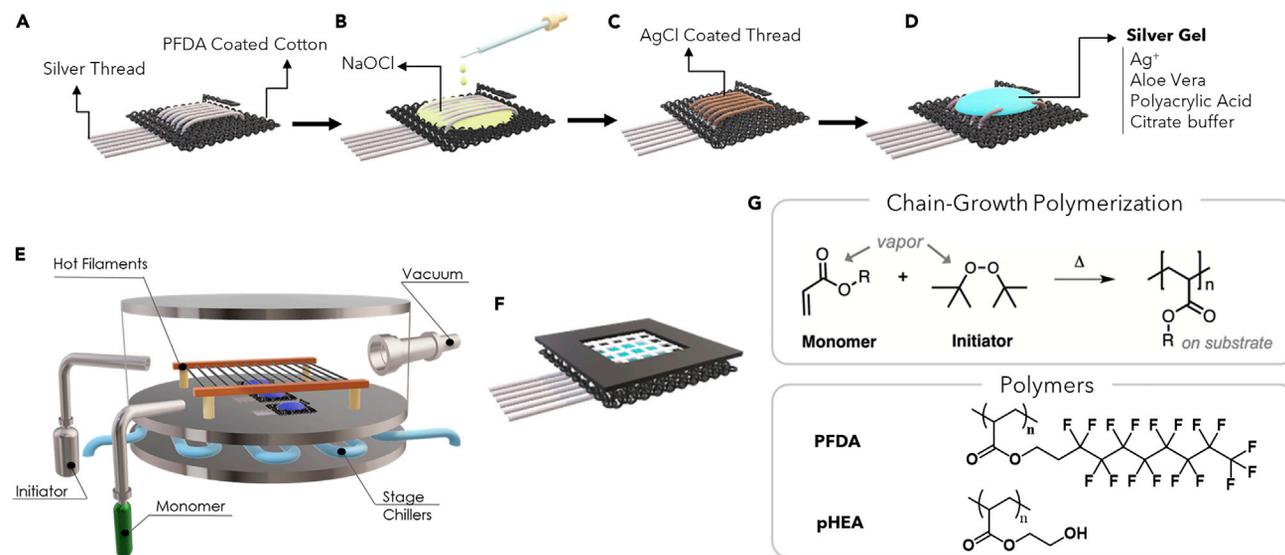
Figure 2. Fabrication of tAgTrode

(A) An array of silver thread is sewn into fabric.

(B and C) (B) Bleach treatment oxidizes the outer surface of the silver thread array and (C) creates a layer of AgCl on the surface of the threads, which acts as an ionic interface for biopotential transduction.

(D–F) (D) A commercial silver gel is applied on the surface, (E) the gel is vapor coated with pHEA using initiated chemical vapor deposition (iCVD), and (F) the gel is gently covered with a PFDA-coated (via iCVD), open-weave cotton fabric and framed with PFDA-coated (via iCVD) cotton flannel to impart mechanical stability.

(G) General polymerization reaction enacted during iCVD (top) and the monomers used in this study (bottom).

biocompatible hydrogel with known uses as a coating for biomedical devices and in drug delivery.[43,45–47] The core idea is that, as pHEA is being synthesized from vaporized monomers and initiators during the iCVD process, superhydrophilic HEA monomers and their low-molecular-weight oligomers will diffuse into the aqueous silver mixture during the polymerization process and afford a highly crosslinked composite hydrogel (Figure 2G). Upon doctor blading a layer of the commercial silver gel onto the bleach-treated tAg array (Figure 2D) and growing a micron-thick coating of pHEA using iCVD, we successfully create a rugged, reusable (rehydratable), and wash-stable solid-state electrolyte on top of our embroidered tAg array. The pHEA layer that is formed via iCVD also grafts onto the PFDA coating on the cotton backing layer, ensuring that the composite hydrogel does not easily peel off from the tAg array. When hydrated, this composite hydrogel mechanically behaves like the foams used in the reference electrodes and is sufficiently cushion-like to minimize motion artifacts in the absence of any harsh skin adhesives.

To complete the fabrication process, we cover the composite hydrogel with a piece of open-weave cotton gauze and frame it with cotton flannel, and subsequently sew these fabric layers together with the PFDA-coated cotton backing layer to isolate the self-contained tAgTrode (Figure 2F). The open-weave cotton gauze covering protects the composite hydrogel from mechanical abrasion during wear while also allowing for rehydrating the gel and direct contact between the hydrogel and a wearer's skin through its wide pores. To prevent the framing and backing fabrics, rather than the hydrogel, from absorbing water/sweat, all the fabrics used in this electrode are rendered hydrophobic by fluoroalkylating with PFDA using iCVD.[48,49] It is also worth mentioning that the cytotoxicity test of both the composite hydrogel electrolyte and PFDA-coated fabric was carried out with zero sensitivity.

Matter
Article

CellPress

Properties of tAgTrode

We studied the hydration-dehydration kinetics of our iCVD-created composite hydrogel by soaking three dry tAgTrodes into reverse osmosis (RO) water and measuring the hydrogel dimensions while keeping track of time. As shown in Figure 3A, we observed that the volume of the hydrogel increased 40-fold in 15 min, which suggests that its swelling kinetics falls in the category of the previously reported[50] highly structured and porous hydrogel films. Once no more observable change was detected in the degree of swelling, we allowed the samples to dry out in the ambient condition while measuring their dimension every hour. As shown in Figure 3B, it took almost 40 h for the composite hydrogel to fully dry out. Furthermore, the tAgTrode withstood more than 30 consecutive hydration-dehydration cycles without any noticeable degradation in the electrical signal.

The presence of Ag^+ cations in the gel provides both ionic conductivity and antimicrobial properties. In fact, these cations are ligated by both citrate anions and anionic acrylate repeat units in the poly(acrylate) component, suggesting that the silver salt is not easily leached out of the formulation. Energy-dispersive X-ray spectroscopy (EDX) and scanning electron microscopy (SEM) confirmed the persistence of silver atoms (i.e., a persistent mixture of Ag^0 and Ag^{+1}) within the hydrogel, even after enduring 15 laundering cycles with laundry detergent (Figures 3C and 3D).

To uncover the fact that tAgTrode performance is effectively independent of the degree of hydration of its constituent hydrogel by either water or perspiration, we performed four-point probe measurements. The data shown in Figure 3E revealed that the resistivity of the tAgTrode dropped steeply when minimally hydrated from a fully dry state, but then remained constant with further addition of either water or saline. This observation verified the user-friendly nature of tAgTrode, since users need not worry about specific hydration requirements for everyday applications. Moreover, it was seen that further increase in the saline does not disturb the resistivity constancy, implying that the electrode performance will not be disturbed if being soaked in users' perspiration.

To probe the operational stability of the tAgTrode during continuous monitoring of physiological signals, we scanned the change in the baseline of its electrical output under the application of constant voltage (0.25 mV) via chronoamperometry. As shown in Figure 3F, the baseline of the electrical output fluctuates less than 4% over the course of a 16-h measurement cycle under ambient conditions, indicating that tAgTrode is well suited for longitudinal monitoring.

To make a primary evaluation of the performance of our electrodes, we used two tAgTrodes placed at the wrists and one at the ankle to measure an ECG signal using a low-cost portable ECG monitoring device (Figure S2). We observed that the ECG signal provided by the tAgTrodes matches that obtained with reference electrodes, confirming that our fabric bioelectrode is a perfect substitute for the conventional adhesive-backed electrodes, while, as depicted in Figures 3G and 3H, their variably patterned arrays can be readily created on different fabrics and easily sewn onto premade garments, allowing for superior integrability over conventional electrodes.

Press-ION Design and Properties

As mentioned before, there is a significant interest in having the capability of contextual measurement of multiple physiological signals simultaneously in a single device. Therefore, we focused on sensors that respond to pressure in order to capture the pressure exerted by blood pulsing through an artery as a complement to eye
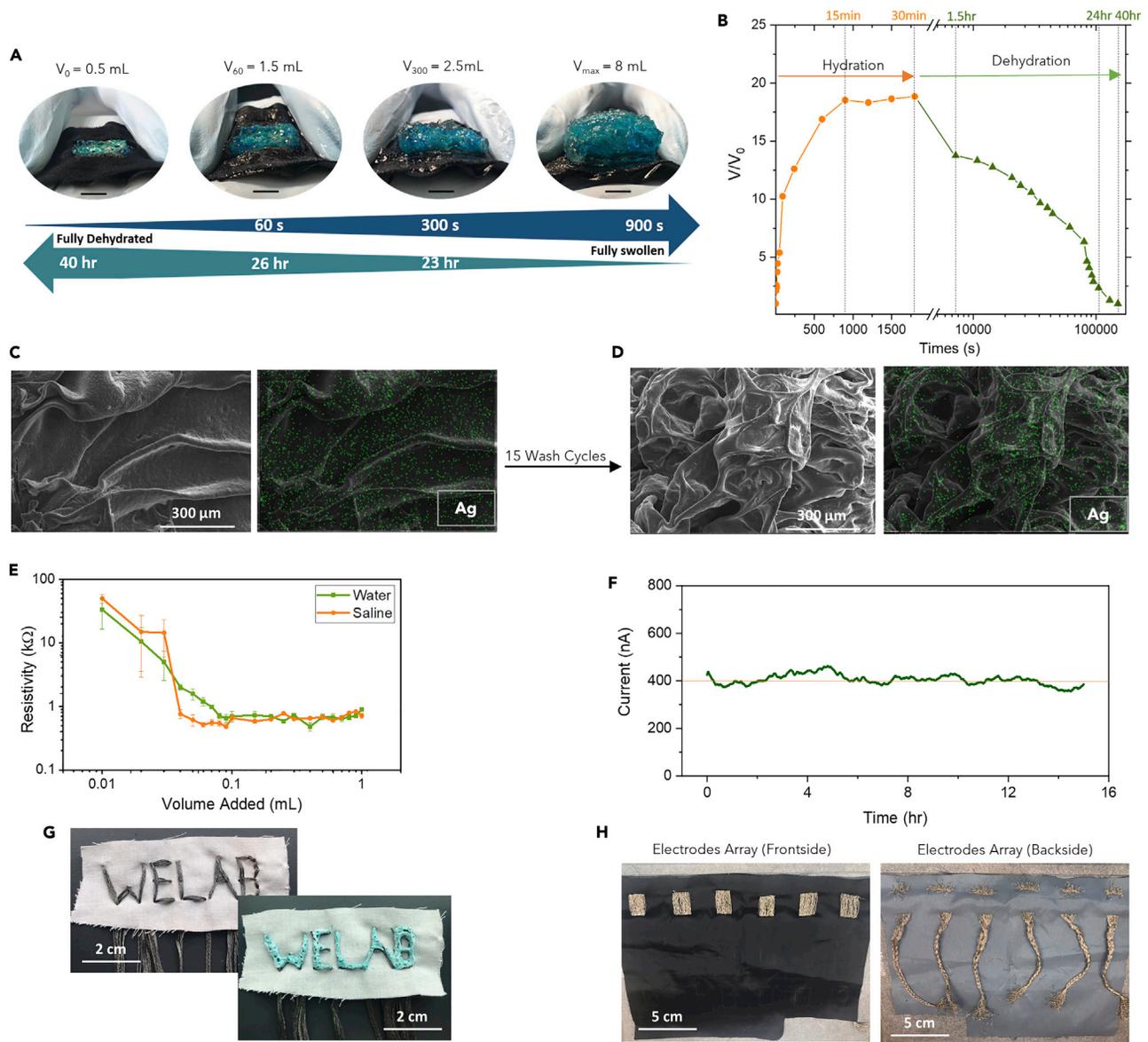
Figure 3. Properties of tAgTrode

(A and B) (A) Images of swelling and (B) kinetics of hydration and dehydration of the hydrogel used in tAgTrode. Scale bars, 5 mm.

(C) SEM image (left) and silver elemental map obtained using EDX (right) of the hydrogel used in tAgTrode.

(D) SEM image (left) and silver elemental map obtained using EDX (right) of the same hydrogel after 15 laundering cycles with laundry detergent.

(E) Change in resistivity of the hydrogel upon the addition of water and saline measured by a four-point probe.

(F) Stability of the electrical signal of the electrode over 16 h measured using chronoamperometry with an applied potential of 0.25 mV.

(G) Photograph of the patterned tAgTrode before (top left) and after application of the hydrogel (bottom right).

(H) Photographs of the front side (left) and back side (right) of an embroidered electrode array to demonstrate scalability.

parameters. We targeted a fabric-based pressure-sensitive patch, called Press-ION, that we previously used[51] to reveal a user's sleep posture, heartbeat, and respiration when embedded into a loose-fitting sleep shirt. As illustrated in Figure 4A, the Press-ION comprised three fabric layers: one ion-conductive cotton interlayer, as the active component, sandwiched between two silver-coated nylon swatches that served as the plate electrodes. The ion-conductive layer was created by coating a porous, medium-density cotton fabric with a polysiloxane polymer containing a
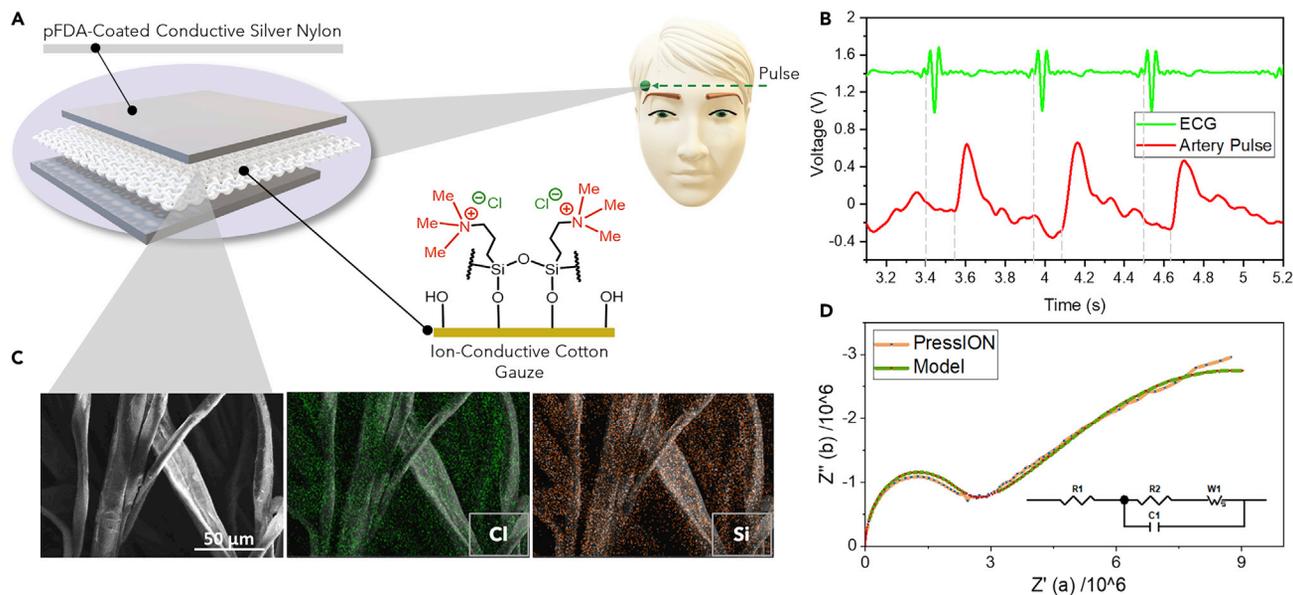
Matter
Article

CellPress

Figure 4. Structure and Properties of Press-ION

(A) Schematic of Press-ION.

(B) Pulse waveform recorded by gently placing the Press-ION over the supraorbital artery of a user. The pulse waveform provided by the Press-ION is compared with a ground-truth ECG signal recorded at the same time. The time lag between the pulse waveform recorded by the Press-ION and the ECG signal is 140 ms, which corresponds to the travel time needed for blood to reach the supraorbital artery after a heart beat.

(C) SEM images and elemental EDX maps for the active layer of Press-ION, indicating uniform coating, the presence of chlorine atoms, and the presence of silicon atoms on the surface, respectively, from left to right.

(D) Measured impedance of Press-ION and the predicted impedance for the equivalent circuit model shown as an inset. This Nyquist plot reveals the significant contribution of ionic conductivity in the pressure sensor.

cationic quaternary ammonium moiety and a chloride counterion, which is biocompatible. The quaternary ammonium moiety remains immobilized on the surface of the cotton fabric, while the biocompatible chloride counterion is mobile and gives rise to an evident ionic conductivity. SEM imaging and EDX mapping confirmed that the polysiloxane exclusively formed a surface coating around the cotton fabric and did not soak into its constituent fibers (Figure 4B). The functionalized ion-conductive layer was further encapsulated with a poly(perfluoroalkylsiloxane) coating through iCVD. As previously reported, the hydrophobic nature of this coating protects the ion-conducting fabric against common aging processes, such as erosion during laundering or air oxidation, ensuring that the ionic conductivity of the sensor will not be washed away or diluted if the Press-ION comes into contact with sweat.

Regarding the working principle of Press-ION, under the application of an inward pressure, three simultaneous phenomena take place.[51] First, due to a putative decrease in the air gap between the two charge collectors, the number of available ion-percolation pathways across the surfaces of the two functionalized cotton interlayers increases. Second, the overall thickness of the fabric decreases, which leads to a change in the capacitance of the sensor. At the same time and as the third phenomenon, the applied pressure results in the relocation of the mobile chloride ions and a corresponding piezoionic effect. All of these processes contribute to the reduction in impedance of the Press-ION upon the application of pressure.[51] Impedance spectroscopy of the patch provided further insight into the working mechanism of this sensor. The data shown in the Nyquist plot (Figure 4D) can be described well by

CellPress

an equivalent circuit model containing a capacitive and ion-conductive Warburg element, where the semicircle part of the data was indicative of a finite-length Warburg impedance with resistance cutoff in the low-frequency region. These data form a typical illustration[52,53] of combined resistive sensitivity at high frequency and diffusional ion transfer at lower frequencies.

By stitching the Press-ION onto the eye mask in the supraorbital position (Figure 4B), we observed that the pressure exerted on the patch by blood pulsing through the supraorbital artery is sufficiently strong to yield a clear voltage response. The signal output of the Press-ION was an ideal pulse waveform, the validity of which was confirmed by separately and simultaneously measuring a ground-truth ECG signal. To the best of our knowledge, this is the first fabric-based device capable of sensing an artery pulse signal, which, by further appropriate signal processing, can yield cardiac rhythm and other useful physiological information.

Integration of Sensing Elements into Eye Mask

Our bimodal eye mask (Chesma) incorporates four tAgTrodes in four periorbital positions along the right and left eye sockets, one reference tAgTrode located in the top center of the eye mask (on the forehead), and one Press-ION pulse detector at the supraorbital artery position (Figure 1D). All six of these fabric electrodes are tightly sewn onto a commercially available, fabric-covered, molded foam sleep mask, chosen because it is lightweight and adaptable to a wide variety of head shapes and sizes. As shown in Figure 1C, silver-plated nylon threads, cladded with a nanoscale (40–50 nm) coating of a hydrophobic polymer, PFDA, and encased within cotton piping, serve as lightweight, flexible, and laundering-stable[48] interconnects between the six sewn-on electrodes and two printed circuit board (PCB) microcontrollers (MCUs) (Figures 1E and 1F). Though rigid, these PCBs have a small form factor and are the same width as the eye mask's elastic band; therefore, we are able to simply hide these rigid components in the elastic band of the eye mask without significantly compromising the overall comfort level. A movie of a user wearing the final, portable product with imperceptibly integrated wires and PCBs is presented in Video S1.

System Design and Data Acquisition

Chesma captures two signals, EOG and pulse, which required slightly different data-acquisition pipelines. We describe each of these in turn (Figure 5A).

EOG Data Acquisition

There were several constraints on designing an amplification board for EOG applications in the context of a wearable device. First, the amplitude of the desired EOG signal was on the order of 10 μV, which was below the minimum detectable voltage swing for low-power analog-to-digital converters (ADCs). To solve this issue, we designed and implemented an amplifier board to magnify the EOG signal so that the low-power ADCs could capture this signal of interest. The board contained two channels for vertical and horizontal signals. For the vertical channel, signals from two vertical electrodes were fed to a differential amplifier. For the horizontal channel, the outputs from the differential amplifiers were further passed through two stages of amplification and filtering to increase the SNR. To synchronize the body potential with the analog board and reduce the noise power, we connected the middle electrode to the ground of the circuit.

Second, the DC baseline for the EOG measurement varied according to various physical conditions, such as the impedance match between the five tAgTrodes,
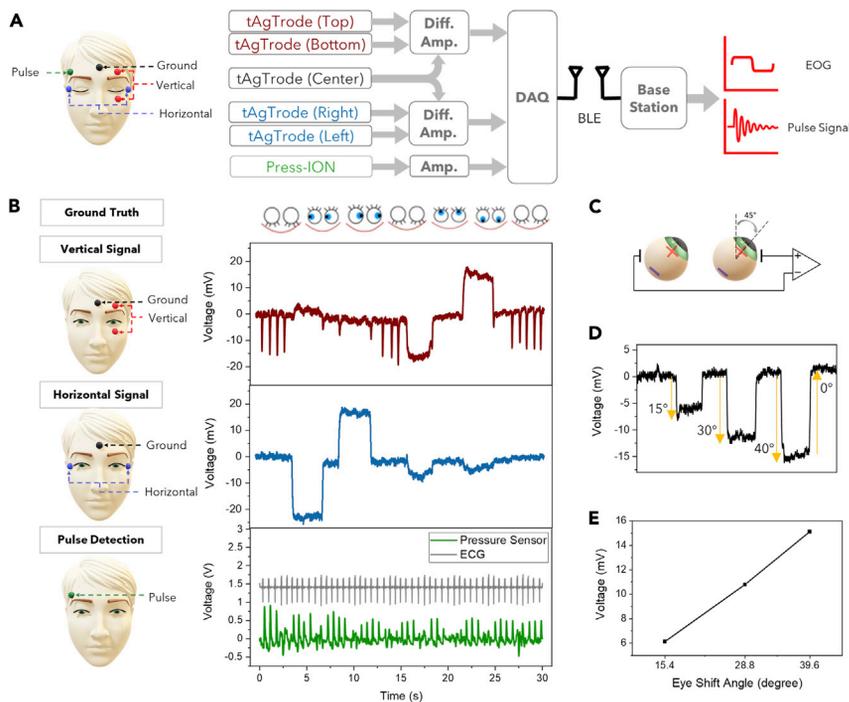
CellPress

Figure 5. Representative Dataset Generated by Chesma

(A) A flowchart that describes the data-acquisition pipeline in Chesma.

(B) Respectively from top to bottom, cartoons indicating the eye movement or blinking action performed, signals acquired from the vertical and horizontal tAgTrodes with each movement, and pulse waveforms acquired from the Press-ION verified by a ground-truth ECG signal.

(C) Schematic to describe the working principle of EOG in ocular angle detection.

(D) Observed electrical signal with varying ocular angle.

(E) Observed voltage versus ocular angle showing linearity up to 40°.

pressure on the skin surface, and changing skin conductivity during use. As a result of this varying DC baseline, the gain of the electronic circuit could not exceed certain values to avoid voltage saturation at the output of the board. This issue could not be handled by DC-rejection methods, since the DC portion of the signal contains information regarding eyeball gaze direction. Consequently, we limited the gain of the electronics board to 30 (v/v).

Pulse Data Acquisition

To capture pulse waveforms from the supraorbital artery, we needed to amplify the raw output of the Press-ION. A second electronic board was designed to amplify the frequency components in the range of 2–10 Hz, which covered the strongest components of heartbeat pulses. This board was connected to the pressure sensor and amplified the signal up to 400 times to capture tiny pressure changes due to heartbeat. It consisted of a unity-gain amplifier to isolate the sensor, followed by a three-stage inverting active filter.

Wireless Data Transmission

Once the sensor data was acquired, data needed to be processed and communicated. Our design transmitted raw data to cloud processing and data visualization. Since the overall system is required to have a small form factor and low power consumption, we chose the BL652 integrated circuit containing microcontroller and Bluetooth low-energy (BLE) radio. The BLE client—a laptop computer in our

setup—read the value of the characteristics and received the sampled data. The BLE radio transmitted packets of 10-ms intervals and 10 dBm transmit power, which leads to 3.5 mA of current consumption. The power consumption of BLE was directly related to the number of packet transmissions per second and could be reduced by batching data and transmitting less frequently. Taken together, the MCU and BLE consumed 10 mW of power, and the analog amplifiers consumed a total of 1.5 mW.

Validating Chesma Performance

To validate the performance of Chesma, we asked a participant to sit at rest with the face 20 inches away from a 22-inch monitor and to follow a white ball moving on the black background of the monitor by just moving the eyes. The experiment consisted of 20 vertical and 20 horizontal eye movements with a velocity of 22°/s and 28°/s and maximum distances of 15° and 26°, respectively. Movies of the electrical signal produced upon a wearer moving the eyes in the vertical and horizontal directions are provided in Videos S2 and S3, respectively. The relative voltage to the actual eye positions was plotted in Figure 5B for the horizontal and vertical channels in a 30-s time interval, and simultaneously the voltage sensed via artery pulse was validated via standard ECG measurement.

To confirm that the voltage output of the Chesma was linear with the angle of the user's gaze, we asked a participant to sit with the face 20 inches away from a monitor and look straight at a white ball in the middle of the screen. The participant was asked to remain as stationary as possible and to follow the ball by just moving the eyes as the ball moved back and forth to three fixed distances, at 15°, 30°, and 40°. Figure 5D shows the horizontal EOG signal acquired during the experiment. The relative voltage to the actual eye positions is plotted in Figure 4E, where it can be seen that the curve represents a perfect linear relationship. Consistent with previous EOG studies,[54–56] Figure 5E reveals that the relationship between the eye angle and the amplitude of the measured EOG voltage signal was linear, up to 40°, which makes it quite useful for human-computer interface applications.[56,57]

tAgTrode Outperformance Compared with Other Electrodes

The most distinguishing factor in thus-far developed wearable devices for monitoring eye parameters is the effect of ambient electrical noise and motion artifacts, i.e., spurious signal fluctuations caused from even the smallest of head or body movements, on the desired EOG signal. Therefore, in addition to the Chesma prototype with tAgTrodes and Press-ION, we assembled two control eye masks, each containing different electrodes in place of the tAgTrodes: the first control device incorporated the adhesive-backed reference electrode and the second a plain silver-coated fabric lacking a hydrogel electrolyte as the electrode (called the "dry electrode"). The signal power for each of the three devices was computed using Equation 1:

$$\text{Signal Power} = \frac{1}{T}\sum_{t=0}^{T} v(t)^2, \qquad \text{(Equation 1)}$$

where T represents the time period of the action and $v(t)$ denotes the voltage magnitude of the signal at time instance t. The procedure was repeated for each of the three types of electrodes mounted on the eye mask, the result of which can be seen in Figure 6A, suggesting almost the same signal power in all cases. We then compared different electrodes with respect to the SNR, defined by Equation 2:

$$\text{Signal-to-Noise Ratio (SNR}_{dB}) = 10\log_{10}(\text{Signal Power}) - 10\log_{10}(\text{Noise Power}),$$
$$\text{(Equation 2)}$$

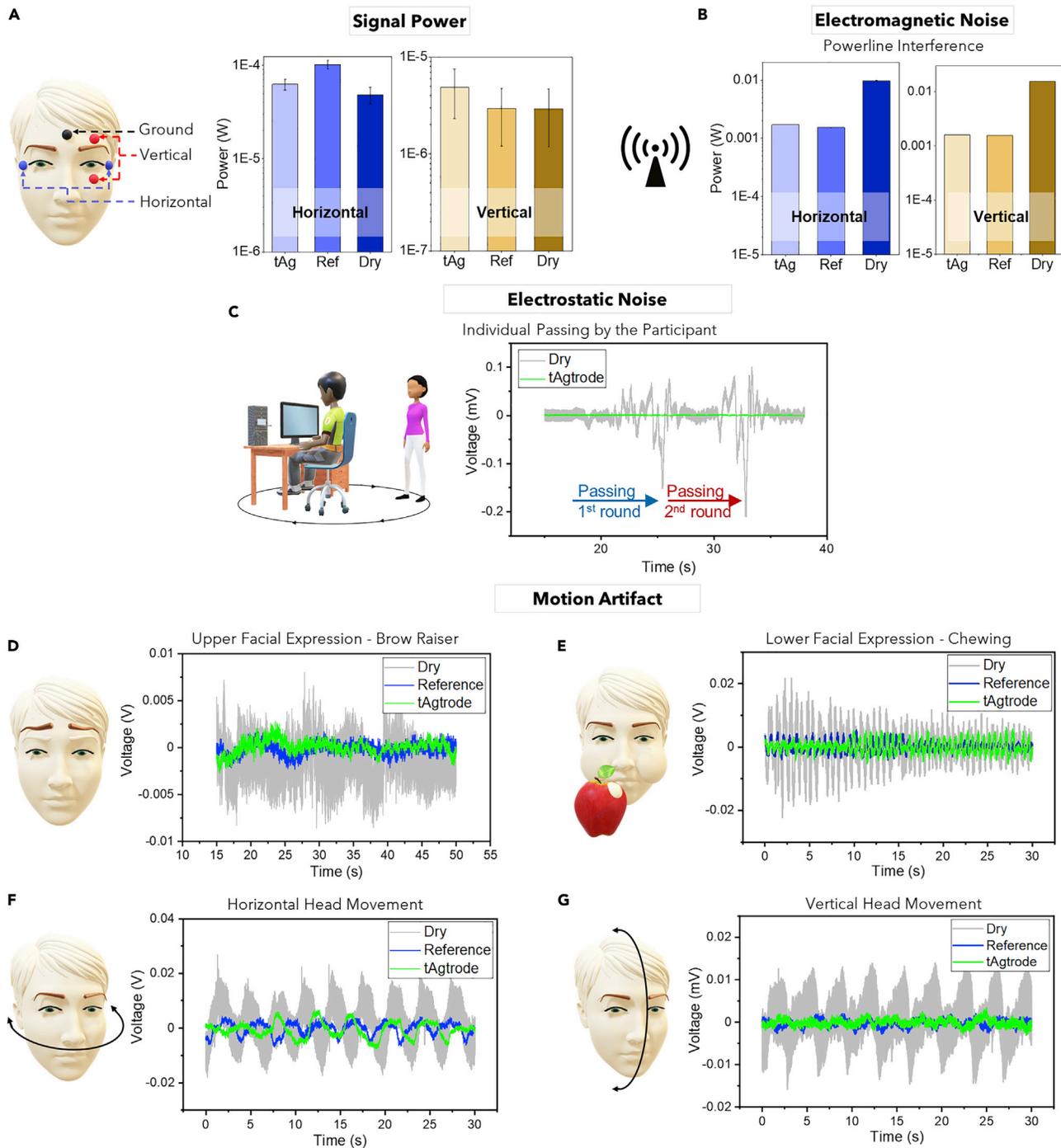**Matter**
Article

CellPress

Figure 6. Comparison Between tAgTrode, Dry Silver Electrodes (Dry), and Commercial Electrodes (Reference) for Recording EOG Data

(A and B) (A) Desired signal power and (B) noise power generated due to ambient electromagnetic interference for horizontal (left) and vertical (right) channel electrodes, respectively.

(C–G) (C) Noise power generated by perambulating within 10 feet of the Chesma user. Real-time EOG signals recorded while performing prescribed motions, specifically (D) brow raise, (E) chewing food, (F) horizontal head movement, and (G) vertical head movement, showing the electrical noise generated due to motion artifacts. In all cases, tAgTrodes displayed the highest signal-to-noise ratios.

Table 1. Summary of Signal-to-Noise Ratios Demonstrated by Three Different Electrodes

| Sample | Electrostatic | Electromagnetic | Motion Artifact | | | | |
| | Powerline | Passing Person | Talking | Chewing | Brow Raise | Head Movement | |
						Horizontal	Vertical
tAgTrode	18.31	14.11	12.81	9.78	−6.08	8.04	5.89
Dry electrode	−2.62	−16.43	2.17	1.63	−12.46	−1.80	−5.04
Ref. electrode	21.04	16.31	18.90	11.64	−4.63	10.15	17.41

where signal power is calculated using Equation 1. The summary of the comparison between three different electrodes based on SNR is reported in Table 1. In general, a larger SNR means a higher signal power relative to the noise power. If the spurious signal from a particular noise source is stronger than the EOG signal (such as in the case of the brow-raise study), a negative SNR value will be obtained.

To examine how the electromagnetic field of ubiquitous power lines affects the EOG signal (Figure 6B), we collected non-activity data, whereby we asked the participant to sit still in a cubicle inside an office room on the UMass Amherst campus while staring at a mark placed on a wall. The room was chosen because it contained multiple functioning desktop workstations and power lines inside its walls. We then removed the blinks from the EOG signal to provide the "none" label and calculated the noise power with the assumption that now the signal only contains powerline interferences. As seen in Figure 6B and reported in Table 1, the SNR for tAgTrode is ~20 dB higher than the dry one. Next, we asked the participant to remain stationary as in the aforementioned setup and asked one other person to walk around the participant twice. In this experiment, we wanted to analyze how electrostatic noises can affect each of these electrodes (Figure 6C), whereby we observed ~30 dB increase in SNR as compared with dry electrodes.

Finally, to study the effect of regular body movement and facial expressions on the EOG signal, we performed the same horizontal/vertical eye movement test in four different conditions: horizontal and vertical head movement, chewing, and talking, the details of which can be found in Experimental Procedures. The relative voltages corresponding to EOG signals captured in these experiments are shown in Figures 6D–6G. These results confirmed the significant role of our hydrogel electrolyte in noise reduction, even in the absence of any adhesives on the skin.

Longitudinal Performance, Aging Behavior, and Wash Stability

For the longitudinal study, our goal is to compare the captured EOG signal strength during the continuous long-term wearing of our electrodes. To this end, we designed a simple experiment and asked a participant to perform it every 30 min. The experiment consists of 20 vertical and 20 horizontal eye movements with a velocity of 22°/s and 28°/s and the maximum distances of 15° and 26°, respectively. As shown in Figure 7A, both the horizontal and vertical signals do not display any degradation even after 6 h of being continuously used by the wearer without any rehydration, which suggests the capability of this device to be used for long-term applications. The data illustrate the effect of up to 15 laundry cycles on the electrode performance.

It is significantly important to minimize the contact impedance mismatch between the electrodes in function.[58] In fact, one of the main sources of motion artifacts in EOG is skin deformation arising from changes in the thickness of the epidermal layer
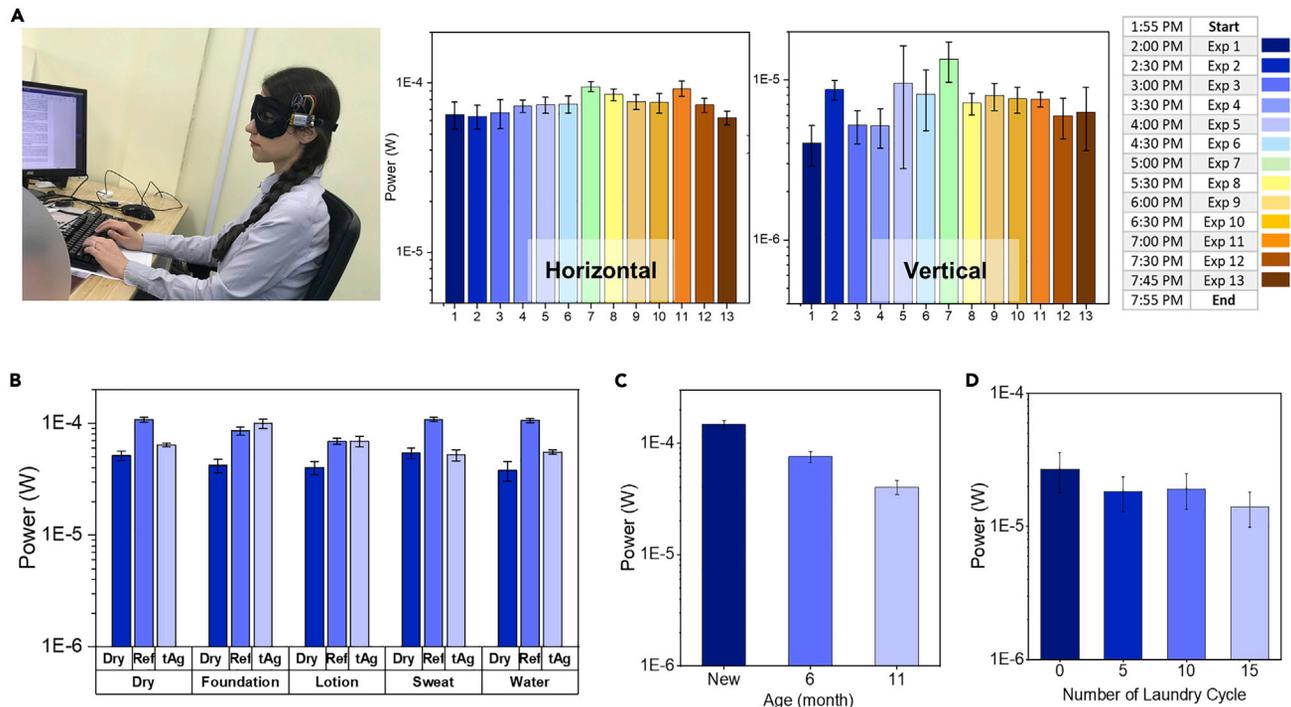
Matter
Article

CellPress

Figure 7. Longitudinal Acquisition of Physiological Signals from the Face Using Chesma
(A) Data obtained over 6 h of continuous use of Chesma in an office for both horizontal and vertical eye movement.
(B) Signal power produced by users with varying skin conditions.
(C) Signal power observed after aging Chesma for 6 and 11 months.
(D) Signal power observed after laundering Chesma with detergent.

across different parts of the face and various skin conditions.[59] For this reason, skin preparation is a dire necessity in using commercial reference electrodes—such as shaving, applying alcohol on the skin to clean the area, and even abrading with sandpaper to decrease the thickness of the dead layer of skin. However, tAgTrode is designed to be applied without any skin preparation, and, interestingly enough, as the water soaks into the skin it renders the stratum corneum less resistive, which is why the signal gets even better in long-term applications (Figure 7A). To evaluate the effect of the skin condition on the EOG signal strength, we asked the participant to repeat the same horizontal/vertical eye movement experiment for four different skin conditions: bare skin, sweaty, with lotion, and with make-up foundation. According to Figure 7B, the skin condition shows less to no effect on the signal amplitude.

In addition to a longitudinal study, it is crucial for a long-term health-monitoring device to be functional in a long period of time. Thus, we studied the effect of aging on the electrodes by measuring the eye movement signal from the same subject and with the same experimental setup after intervals of 6 and 11 months. The data revealed in Figure 7C show that the signal shows a constancy in strength, with no noticeable degradation over almost a year, which is a promising result for further commercialization of the product.

Regarding the wash stability of the electrodes, the electrical performance of the electrodes was studied by measuring the signal strength of EOG data after 5, 10, and 15 home-laundering cycles. As shown in Figures 7A and 7C, a very slight change

CellPress

is observed in the signal strength of the electrodes after being washed, which bears testimony that the electrodes can withstand at least 15 home-laundering operations.

Conclusion

We present a one-of-a-kind fabric-based wet electrode design and an integrated wearable system (Chesma) for wireless monitoring of eye parameters and artery pulse, simultaneously, over prolonged periods. The silver-thread-based electrode (tAgTrode) successfully overcomes all the drawbacks of commercial wet electrodes such as aesthetic issues, discomfort, and wash stability, while maintaining high and constant SNRs during repeated, longitudinal applications. They also can be embedded into a variety of wearable platforms by further miniaturization if desired. This capability allows us to integrate these electrodes into a lightweight and portable eye mask for EOG data acquisition. Furthermore, an all-fabric ionic pressure sensor (Press-ION) is integrated into the eye mask to capture artery pulse waveforms as a complementary physiological signal. We anticipate that this unique bimodality of Chesma and its ability to track the pulse along with eye movement will enable a host of cutting-edge biomedical, psychological, and psychosocial studies, in addition to improving the responsiveness of gaming and AR/VR headsets.

EXPERIMENTAL PROCEDURES

Resource Availability

Lead Contact

Trisha L. Andrew, tandrew@umass.edu.

Materials Availability

The electrodes and sensing platforms described in this study will be made available on request, but we may require a payment and/or a completed Materials Transfer Agreement if there is potential for commercial application.

Data and Code Availability

The published article includes all EOG data generated or analyzed during this study.

Materials

Monomers HEA and 1H,1H,2H,2H-perfluorodecylacrylate (PFDA; 97%), and the initiator *tert*-butyl peroxide (TBPO; 98%) were purchased from Sigma-Aldrich and used without further purification. Trichloro-(1H,1H,2H,2H-perfluorooctyl)-silane and *N*-(3-(trimethoxysilyl)-propyl)-*N,N,N*-trimethylammonium chloride (15 vol % in isopropanol) were purchased from Gelest and used without further purification.

Fabrication of tAgTrode

Preparation of the Electrode Plate

The platform for each electrode was a PFDA-coated cotton fabric. Cotton fabrics (purchased as bolts from Joanne Fabrics) were cut into 2×3-cm^2 swatches that were sonicated in deionized water for 15 min, rinsed with isopropanol, and dried in air. These swatches were placed inside a custom-built iCVD reactor and coated with a micron-thick layer of PFDA. On the center of each of these PFDA-coated swatches, an array of approximately 50 silver-coated nylon threads (tAgs, purchased from LessEMF) was embroidered into a 1×1.5-cm^2 rectangular shape. To create a silver(I) chloride layer on the surface of the tAg array, we dropped 1 mL of commercial laundry bleach (10 wt % NaOCl in water) onto the front face of silver thread embroidery pattern such that the entire surface was covered. The bleach solution was left on the surface of the silver threads for 40–50 s and then rinsed away with deionized water.

⌀ CellPress

Synthesis of the Composite Hydrogel Electrolyte

For all the electrodes used in this study, 0.4 mL of a commercial silver gel formulation (MyDoctorSuggest, composed of water, Carbopol, sodium bicarbonate, aloe vera, citrate buffer, and silver(I) chloride) was doctor bladed onto the bleach-treated tAg array. Because the PFDA-coated backing cotton platform was hydrophobic, the silver gel automatically localized over the hydrophilic tAg array during the doctor-blading process. These gel-coated samples were immediately placed inside a custom-built iCVD reactor (stainless-steel walls, 290 mm diameter, 70 mm height) inside which the polymerization of HEA was carried out under vacuum. The reactor included separate monomer and initiator inlets, cooling tubes to control the temperature of the stage, and heating filaments that cleaved the TBPO initiator to form the reactive radicals that initiate the chain-growth polymerization reaction. HEA was vaporized outside the reactor at 110°C and introduced into the chamber, where it reacted with initiator radicals and polymerized. The deposition was conducted for 60 min at a constant pressure of 1 torr. The temperature of the filament and the stage were kept constant at 300°C and 15°C, respectively. To extract residual traces of unreacted HEA monomers in the composite hydrogel, we sequentially soaked the composite hydrogel in isopropanol and water for 30 min immediately after the iCVD process.

Encapsulation

A 30-min deposition of PFDA using monomer PFDA and initiator TBPO was conducted on prewashed cotton gauze, cotton flannel (purchased from Joanne Fabrics), and silver-coated nylon threads in the same iCVD chamber described above, at a constant pressure of 400 mtorr. PFDA was vaporized at 80°C. All other conditions were the same as those described above for pHEA deposition.

Composite Hydrogel Swelling Kinetics

Three dry tAgTrodes were immersed in RO water until no observable change was detected in the degree of swelling of the samples. The dimensions of the composite hydrogels on the top of tAgTrodes were measured using a caliper as they were swelling. Starting from a completely dehydrated state, a typical sample of the iCVD-created composite hydrogel swells to 1,600% of its initial volume after being soaked in RO water for 15 min. The tAgTrodes were then allowed to dry out at room temperature, in a room with a constant relative humidity of 30%, and their physical dimensions measured every hour. As seen in Figure 3, dehydration of the composite hydrogel was completed after 40 h and the electrodes returned to their initial weight. Importantly, the same response time for hydration/dehydration and associated volume changes were invariably observed for 12 different electrodes, even after more than 20 wetting/drying cycles, implying that these electrodes are highly robust for continued use.

Cytotoxicity Test

The cytotoxicities of both the composite hydrogel electrolyte and PFDA encapsulation were independently assessed *in vitro* using a culture of mouse fibroblast cells (standard L-929) (ATCC CCL-1). The test was carried out by a third-party lab, Nelson Laboratories (Salt Lake City, UT, USA), in accordance with criteria established by US Pharmacopeia and National Formulary (USP 87) and ANSI/AAMI/ISO 10993-5 standards. Results are summarized in Table S1, and raw data from Nelson Laboratories are included at the end of Supplemental Information.

Wash Stability

Each washing cycle equates to 40 min of stirring at 300 rpm in the solution of water and laundry detergent (100:1 [v/v]) at 40°C, followed by rinsing with water for 10 min and being dried at room temperature.

CellPress

Fabrication of Press-ION

The pressure sensor was a 25 × 25-mm^2 patch composed of two layers of ion-conductive cotton gauze sandwiched between two layers of silver-plated nylon fabric. After being sonicated in deionized water for 15 min followed by rinsing with isopropanol, as-purchased cotton gauze was soaked in an isopropanol solution containing N-(3-(trimethoxysilyl)-propyl)-N,N,N-trimethylammonium chloride (15 vol %) for 30 min, followed by 2 h of being cured at 100°C. The functionalized fabric was then rinsed with isopropanol and dried in air overnight. To provide the sensor with wash stability and durability, we performed vapor deposition of trichloro-(1H,1H,2H,2H-perfluorooctyl)-silane performed in the iCVD chamber described above. This deposition was performed at a constant pressure of 1 torr for 30 min. The functionalized layers of cotton gauze were then cut into two 25 × 25-mm^2 swatches, each of which was individually sewn onto a 20 × 20-mm^2 sheet of silverized nylon (LessEMF). The final four-layer pressure sensor was produced by sewing together these two joint sheets around the perimeter.

Chemical and Electric Characterization

The surface component and valence state of the electrode plate was studied through XPS (Axis Ultra DLD). The stability of the electrode resistance over time was confirmed through three-electrode chronoamperometry by using a Wavenow potentiostat from Pine Instruments. The resistivity of the hydrogel was studied using a four-point-probe measurement station equipped with an SP4 probe (Pro4-440N, Lucas Labs). The radius of tungsten-carbide tips was 0.04 mm, and the relative distance between them was 1.27 mm.

Impedance spectroscopy was carried out with an Agilent 4294A impedance analyzer. The drive voltage was 600 mV, and the frequency swept from 0.1 Hz to 0.3 MHz. Data fitting and equivalent circuit modeling were conducted by ZView2 software (Princeton Applied Research). Field-emission SEM and EDX spectroscopy were performed with a Magellan 400 microscope.

Performance and Comparison Studies

Talking Study

To analyze the noise over the EOG signal associated to the common lower facial activities such as talking, we asked participants to say out loud the English alphabet twice while being in a stationary position. We asked the participant to avoid any eye movement and stare at a mark placed on a wall at a 1-m distance. The noise power was calculated based on Equation 1, after removing the involuntary blinks from the signal.

Chewing Study

To study the effects of jaw movements, we asked a participant to eat one cup of chopped apples. The participant was asked to remain still and avoid eye movements while staring at a mark on the front wall. The noise power was calculated after removing the involuntary blinks from the signal.

Brow-Raise Study

We made a looped video clip that contains 20 repeating instances of a person raising their eyebrow and provided it to the participant. The participant was asked to perform the facial actions along with the video while being stationary and preventing eye movements.

Matter
Article

ᗒ **CellPress**

Horizontal/Vertical Head Movement Study

Motions of the head induce force at the point of contact of the electrode and the skin, which in turn causes the skin to be compressed, which changes the coupling potential and, thus, the electrical potential measured by EOG. The goal here is to compare the motion artifact on each of these electrodes. To capture the pure motion artifact and eliminate involuntary eye movements, we asked the participant to put on a hat with a long bill and stare at a mark on the edge of the bill while moving the head horizontally and vertically. We did not ask participants to close their eyes as we realized that it is more difficult to control eye movements with closed eyes.

AUTHOR CONTRIBUTIONS

S.Z.H. developed vapor deposition protocols, created fabric-based electrodes, processed data, and helped write the manuscript. S.R. collected physiological signals from the completed device and processed data. A.K. designed the microcontrollers for each type of electrode. X.C. designed the wireless communication component. E.T.A. validated vapor deposition protocols, mass-produced fabric-based electrodes, and helped create prototypes. D.G. and T.L.A. conceived the idea, raised funds, and directed the project. T.L.A. designed and identified materials for the two fabric-based electrodes and the final garment, helped with data analysis, and wrote and edited the manuscript.

DECLARATION OF INTERESTS

The authors declare no competing interests.

REFERENCES

1. Meng, K., Zhao, S., Zhou, Y., Tan, X., Yang, J., Chen, J., Wu, Y., Zhang, S., He, Q., Wang, X., et al. (2020). A wireless textile-based sensor system for self-powered personalized health care. Matter *2*, 896–907.

2. Zhang, N., Huang, F., Zhao, S., Nie, Y., Chen, J., and Fan, X. (2020). Photo-rechargeable fabrics as sustainable and robust power sources for wearable bioelectronics. Matter *2*, 1260–1269.

3. Chen, G., Li, Y., Bick, M., and Chen, J. (2020). Smart textiles for electricity generation. Chem. Rev. *120*, 3668–3720.

4. Majumder, S., Chen, L., Marinov, O., Chen, C.H., Mondal, T., and Jamal Deen, M. (2018). Noncontact wearable wireless ECG systems for long-term monitoring. IEEE Rev. Biomed. Eng. *11*, 306–321.

5. Weder, M., Hegemann, D., Amberg, M., Hess, M., Boesel, L.F., Abächerli, R., Meyer, V.R., and Rossi, R.M. (2015). Embroidered electrode with silver/titanium coating for long-term ECG monitoring. Sensors (Switzerland) *15*, 1750–1759.

6. Kim, T., Park, J., Sohn, J., Cho, D., and Jeon, S. (2016). Bioinspired, highly stretchable, and conductive dry adhesives based on 1D-2D hybrid carbon nanocomposites for all-in-one ECG electrodes. ACS Nano *10*, 4770–4778.

7. Gruetzmann, A., Hansen, S., and Müller, J. (2007). Novel dry electrodes for ECG monitoring. Physiol. Meas. *28*, 1375–1390.

8. Takamatsu, S., Lonjaret, T., Crisp, D., Badier, J.M., Malliaras, G.G., and Ismailova, E. (2015). Direct patterning of organic conductors on knitted textiles for long-term electrocardiography. Sci. Rep. 5, https://doi.org/10.1038/srep15003.

9. Sinha, S.K., Noh, Y., Reljin, N., Treich, G.M., Hajeb-Mohammadalipour, S., Guo, Y., Chon, K.H., and Sotzing, G.A. (2017). Screen-printed PEDOT:PSS electrodes on commercial finished textiles for electrocardiography. ACS Appl. Mater. Interfaces *9*, 37524–37528.

10. Bihar, E., Roberts, T., Saadaoui, M., Hervé, T., De Graaf, J.B., and Malliaras, G.G. (2017). Inkjet-printed PEDOT: PSS electrodes on paper for electrocardiography. Adv. Healthc. Mater. 6, 1601167.

11. Pani, D., Achilli, A., and Bonfiglio, A. (2018). Survey on textile electrode technologies for electrocardiographic (ECG) monitoring, from metal wires to polymers. Adv. Mater. Technol. 3, 1800008.

12. Ramasamy, S., and Balan, A. (2018). Wearable sensors for ECG measurement: a review. Sens. Rev. 38, 412–419.

13. Golparvar, A.J., and Kaya Yapici, M. (2017). Wearable graphene textile-enabled EOG sensing. Proc. IEEE Sensors 2017, https://doi.org/10.1109/ICSENS.2017.8234242.

14. Liang, S., Kuo, C., Lee, Y., Lin, W., Liu, Y., Chen, P., Cherng, F., and Shaw, F. (2015). Development of an EOG-based automatic sleep-monitoring eye mask. IEEE Trans. Instrum. Meas. 64, 2977–2985.

15. Kanoh, S., Ichi-Nohe, S., Shioya, S., Inoue, K., and Kawashima, R. (2015). Development of an eyewear to measure eye and body movements. Proc. Annu. Int. Conf. IEEE Eng. Med. Biol. Soc. EMBS 2015, 2267–2270.

16. Alba, N.A., Sclabassi, R.J., Sun, M., and Cui, X.T. (2010). Novel hydrogel-based preparation-free EEG electrode. IEEE Trans. Neural Syst. Rehabil. Eng. 18, 415–423.

17. Lin, C., Liao, L., Liu, Y., Wang, I., Lin, B., and Chang, J. (2011). Novel dry polymer foam electrodes for long-term EEG measurement. IEEE Trans. Biomed. Eng. 58, 1200–1207.

18. Crea, S., Nann, M., Trigili, E., Cordella, F., Baldoni, A., Badesa, F.J., Catalán, J.M., Zollo, L., Vitiello, N., Aracil, N.G., et al. (2018). Feasibility and safety of shared EEG/EOG and vision-guided autonomous whole-arm exoskeleton control to perform activities of daily living. Sci. Rep. 8, https://doi.org/10.1038/s41598-018-29091-5.

19. Chi, Y.M., Jung, T.P., and Cauwenberghs, G. (2010). Dry-contact and noncontact biopotential electrodes: methodological review. IEEE Rev. Biomed. Eng. 3, 106–119.

20. Yao, S., Swetha, P., and Zhu, Y. (2018). Nanomaterial-enabled wearable sensors for healthcare. Adv. Healthc. Mater. 7, https://doi.org/10.1002/adhm.201700889.

21. Acar, G., Ozturk, O., Golparvar, A.J., Elboshra, T.A., Böhringer, K., and Kaya Yapici, M. (2019). Wearable and flexible textile electrodes for biopotential signal monitoring: a review. Electron 8, https://doi.org/10.3390/electronics8050479.

22. Bulling, A., Roggen, D., and Tröster, G. (2009). Wearable EOG goggles: seamless sensing and context-awareness in everyday environments. J. Ambient Intell. Smart Environ. 1, 157–171.

23. Vidal, M., Turner, J., Bulling, A., and Gellersen, H. (2012). Wearable eye tracking for mental health monitoring. Comput. Commun. 35, 1306–1311.

24. Banerjee, A., Pal, M., Datta, S., Tibarewala, D.N., and Konar, A. (2014). Biomedical Signal Processing and Control Eye movement

sequence analysis using electrooculogram to assist autistic children. Biomed. Signal. Process. Control 14, 134–140.

25. Crawford, T.J., Higham, S., Renvoize, T., Patel, J., Dale, M., Suriya, A., and Tetley, S. (2005). Inhibitory control of saccadic eye movements and cognitive impairment in Alzheimer's disease. J. Biol. Psychiatry 57, 1052–1060.

26. Cruz-Aguilar, M.A., Ramírez-Salado, I., Hernández-González, M., Guevara-Pérez, M.Á., and del Río, J.M. (2020). Melatonin effects on EEG activity during non-rapid eye movement sleep in mild-to-moderate Alzheimer's disease: a pilot study. Int. J. Neurosci. https://doi.org/10.1080/00207454.2020.1750392.

27. Winsky-Sommerer, R., de Oliveira, P., Loomis, S., Wafford, K., Dijk, D.-J., and Gilmour, G. (2019). Disturbances of sleep quality, timing and structure and their relationship with other neuropsychiatric symptoms in Alzheimer's disease and schizophrenia: insights from studies in patient populations and animal models. Neurosci. Biobehav. Rev. 97, 112–137.

28. Danjou, P., Viardot, G., Maurice, D., Garcés, P., Wams, E.J., Phillips, K.G., Bertaina-Anglade, V., McCarthy, A.P., and Pemberton, D.J. (2019). Electrophysiological assessment methodology of sensory processing dysfunction in schizophrenia and dementia of the Alzheimer type. Neurosci. Biobehav. Rev. 97, 70–84.

29. Kumar, D. (2016). Electrooculogram-based Virtual Reality game control using blink detection and gaze calibration. Int. Conf. Adv. Comput. Commun. Inform. 2016, 2358–2362.

30. Xiao, J., Qu, J., and Li, Y. (2019). An electrooculogram-based interaction method and its music-on-demand application in a virtual reality environment. IEEE Access 7, 22059–22070.

31. López, A., Fernández, M., Rodríguez, H., Ferrero, F., and Postolache, O. (2018). Development of an EOG-based system to control a serious game. Meas. J. Int. Meas. Confed. 127, 481–488.

32. Ameri, S.K., Kim, M., Kuang, I.A., Perera, W.K., Alshiekh, M., Jeong, H., Topcu, U., Akinwande, D., and Lu, N. (2018). Imperceptible electroculography graphene sensor system for human-robot interface. npj 2D Mater. Appl. 2, https://doi.org/10.1038/s41699-018-0064-4.

33. Avenel-Audran, M., Goossens, A., Zimerson, E., and Bruze, M. (2003). Contact dermatitis from electrocardiograph-monitoring electrodes: role of p-tert-butylphenol-formaldehyde resin. Contact Dermatitis 48, 108–111.

34. Golparvar, A.J., and Yapici, M.K. (2018). Electroculography by wearable graphene textiles. IEEE Sens. J. 18, 8971–8978.

35. Arnin, J., Anopas, D., Horapong, M., Triponyuwasi, P., Yamsa-Ard, T., Iampetch, S., and Wongsawat, Y. (2013). Wireless-based portable EEG-EOG monitoring for real time drowsiness detection. 35th Annual International Conference of the IEEE Engineering in Medicine and Biology Society (EMBC), 4977–4980.

36. Rostaminia, S., Lamson, A., Maji, S., Rahman, T., and Ganesan, D. (2019). W!NCE: unobtrusive sensing of upper facial action units

with EOG-based eyewear. Proc. ACM Interact. Mob. Wearable Ubiquitous Technol. 3, https://doi.org/10.1145/3314410.

37. Penzel, T., Kantelhardt, J.W., Lo, C.C., Voigt, K., and Vogelmeier, C. (2003). Dynamics of heart rate and sleep stages in normals and patients with sleep apnea. Neuropsychopharmacology 28, S48–S53.

38. Medeiros, M.A., Lins-Filho, O.L., Patriota, T.L.G.C., del Castillo, J.M., Silveira, C.A.M., de Albuquerque, E.S., Montarroyos, U.R., and Pedrosa, R.P. (2020). Abnormal atrial function in hypertensive patients with obstructive sleep apnea assessed by speckle tracking echocardiography. Hypertens. Res. 43, 841–844.

39. Boe, A.J., McGee Koch, L.L., O'Brien, M.K., Shawen, N., Rogers, J.A., Lieber, R.L., Reid, K.J., Zee, P.C., and Jayaraman, A. (2019). Automating sleep stage classification using wireless, wearable sensors. npj Digit. Med. 2, https://doi.org/10.1038/s41746-019-0210-1.

40. Mokhlesi, B., and Varga, A.W. (2018). Obstructive sleep apnea and cardiovascular disease. REM sleep matters! Am. J. Respir. Crit. Care Med. 197, 554–556.

41. Koo, D.L., Nam, H., Thomas, R.J., and Yun, C.H. (2018). Sleep disturbances as a risk factor for stroke. J. Stroke 20, 12–32.

42. Chouchou, F., and Desseilles, M. (2014). Heart rate variability: a tool to explore the sleeping brain? Front. Neurosci. 8, https://doi.org/10.3389/fnins.2014.00402.

43. Gupta, M., Kapur, V., Pinkerton, N.M., and Gleason, K.K. (2008). Initiated chemical vapor deposition (iCVD) for conformal polymeric nanocoatings for the surface modification of high-aspect-ratio pores. Chem. Mater. 20, 1646–1651.

44. Gleason, K.K. (2019). Organic surface functionalization by initiated CVD (iCVD). In Surface Modification of Polymers: Methods and Applications, J. Pinson and D. Thiry, eds. (Wiley-VCH), pp. 107–134.

45. Siafaka, P.I., Zisi, A.P., Exindari, M.K., Karantas, I.D., and Bikiaris, D.N. (2016). Porous dressings of modified chitosan with poly(2-hydroxyethyl acrylate) for topical wound delivery of levofloxacin. Carbohydr. Polym. 143, 90–99.

46. Gallego Ferrer, G., Soria Meliá, J.M., Hernández Canales, J., Meseguer Dueñas, J.M., Romero Colomer, F., Monleón Pradas, M., Gómez Ribelles, J.L., Pissis, P., and Polizos, G. (2005). Poly(2-hydroxyethyl acrylate) hydrogel confined in a hydrophobous porous matrix. Colloid Polym. Sci. 283, 681–690.

47. Pradas, M.M., Ribelles, J.L.G., Aroca, A.S., Ferrer, G.G., Anton, J.S., and Pissis, P. (2001). Porous poly(2-hydroxyethyl acrylate) hydrogels. Polymer 42, 4667–4674.

48. Wanwong, S., Sangkhun, W., Homayounfar, S.Z., Park, K.-W., and Andrew, T.L. (2019). Wash-stable, oxidation resistant conductive cotton electrodes for wearable electronics. RSC Adv. 9, 9198–9203.

49. Soto, D., Ugur, A., Farnham, T.A., Gleason, K.K., and Varanasi, K.K. (2018). Short-fluorinated iCVD coatings for nonwetting

fabrics. Adv. Funct. Mater. *28*, https://doi.org/10.1002/adfm.201707355.

50. Liu, X., Steiger, C., Lin, S., Parada, G.A., Liu, J., Chan, H.F., Yuk, H., Phan, N.V., Collins, J., Tamang, S., et al. (2019). Ingestible hydrogel device. Nat. Commun. *10*, 493.

51. Kiaghadi, A., Homayounfar, S.Z., Gummeson, J., Andrew, T., and Ganesan, D. (2019). Phyjama: physiological sensing via fiber-enhanced pyjamas. Proc. ACM Interact. Mob. Wearable Ubiquitous Technol. *3*, https://doi.org/10.1145/3351247.

52. Sun, L., Chen, S., Guo, Y., Song, J., Zhang, L., Xiao, L., Guan, Q., and You, Z. (2019). Ionogel-based, highly stretchable, transparent, durable triboelectric nanogenerators for energy harvesting and motion sensing over a wide temperature range. Nano Energy *63*, 103847.

53. Macdonald, D.D. (2006). Reflections on the history of electrochemical impedance spectroscopy. Electrochim. Acta *51*, 1376–1388.

54. Simini, F., Touya, A., Senatore, A., and Pereira, J. (2011). Gaze tracker by electrooculography (EOG) on a head-band 10th International Workshop on Biomedical Engineering, https://doi.org/10.1109/IWBE.2011.6079050.

55. Gu, J.J., Meng, M., Cook, A., and Faulkner, M.G. (2001). A study of natural eye movement detection and ocular implant movement control using processed EOG signals Proceedings 2001 ICRA. IEEE International Conference on Robotics and Automation (Cat. No. 01CH37164)*vol. 2*, 1555–1560.

56. Hossain, M.S., Huda, K., Rahman, S.M.S., and Ahmad, M. (2015). Implementation of an EOG based security system by analyzing eye movement patterns. International Conference on Advances in Electrical Engineering (ICAEE), 149–152.

57. Barbara, N., Camilleri, T.A., and Camilleri, K.P. (2019). EOG-based eye movement detection and gaze estimation for an asynchronous virtual keyboard. Biomed. Signal. Process. Control *47*, 159–167.

58. Ireland, N., Certre, B., Unit, N., and Thomas, C.A. (1996). Factors affecting electrode-gel-skin interface impedance in electrical impedance tomography. Med. Biol. Eng. Comput. *34*, 397–408.

59. Taji, B., Shirmohammadi, S., Groza, V., and Batkin, I. (2014). Impact of skin-electrode interface on conductive textile electrodes. IEEE Trans. Instrum. Meas. *63*, 1412–1422.